Accepted Manuscript

Direct measurements of the magneto-caloric effect of $MnFe_4Si_3$ in pulsed magnetic fields

N. Maraytta, Y. Skourski, J. Voigt, K. Friese, M.G. Herrmann, J. Perßon, J. Wosnitza, S.M. Salman, T. Brückel

PII: S0925-8388(19)32610-6

DOI: https://doi.org/10.1016/j.jallcom.2019.07.113

Reference: JALCOM 51401

To appear in: *Journal of Alloys and Compounds*

Received Date: 30 November 2018

Revised Date: 28 June 2019

Accepted Date: 11 July 2019

Please cite this article as: N. Maraytta, Y. Skourski, J. Voigt, K. Friese, M.G. Herrmann, J. Perßon, J. Wosnitza, S.M. Salman, T. Brückel, Direct measurements of the magneto-caloric effect of $MnFe_4Si_3$ in pulsed magnetic fields, *Journal of Alloys and Compounds* (2019), doi: https://doi.org/10.1016/j.jallcom.2019.07.113.

Direct Measurements of the Magneto-Caloric Effect of $MnFe_4Si_3$ in Pulsed Magnetic Fields

N. Maraytta[a], Y. Skourski[b], J. Voigt[a], K. Friese[a,*], M. G. Herrmann[a], J. Perßon[a], J. Wosnitza[b], S. M. Salman[c] and T. Brückel[a].

[a]Jülich Centre for Neutron Science JCNS-2 and Peter Grünberg Institute PGI-4, JARA-FIT, Forschungszentrum Jülich GmbH, 52425 Jülich, Germany.
[b]Hochfeld-Magnetlabor Dresden (HLD-EMFL) Helmholtz-Zentrum Dresden-Rossendorf, D-01328 Dresden, Germany.
[c]Physics Department, Al-Quds University, Palestine.

Abstract

We have studied the magnetic and magnetocaloric response of $MnFe_4Si_3$ to pulsed and static magnetic fields up to 50 T. We determine the adiabatic temperature change ΔT_{ad} directly in pulsed fields and compare to the results of magnetization and specific heat measurements in static magnetic fields. The high ability of cycling even in fields $\mu_0 H$= 50 T confirms the high structural stability of $MnFe_4Si_3$ against field changes, an important property for applications. The magnetic response to magnetic fields up to $\mu_0 H$= 35 T shows that the anisotropy can be overcome by fields of approx. 4 T.

Keywords: Magnetocaloric effect, $MnFe_4Si_3$, Magnetic measurements, Heat capacity measurements.

1. Introduction

The need to reduce the emission of greenhouse gases leads to a high interest in utilizing alternative refrigeration technologies which can replace existing conventional vapor compression techniques. Magnetic refrigeration as a new solid state cooling technology at room-temperature, with a possible energy saving of 20%-30% could be an option for the refrigeration sector **[1].** The magnetocaloric cooling is an energy-efficient and environmentally friendly technology based on the Magnetocaloric Effect **[2].** The MCE is based on entropy changes of magnetic materials under an applied magnetic field, which lead to a change in the temperature of the material **[3].** The MCE can be characterized by two key values: the temperature change (ΔT_{ad}) in an adiabatic process and the entropy change (ΔS_{iso}) in an isothermal process **[4],** which are related via

$$\Delta T_{ad} = \frac{-T}{C(p,H)} \Delta S \quad \text{.....(1)}$$

*Corresponding author.

E-mail address: k.friese@fz-juelich.de (K. Friese)

So far, most MCE studies have been done by calculating the isothermal entropy change, ΔS_{iso} based on indirect methods **[5, 4].**

Direct measurements of the adiabatic temperature change (ΔT_{ad}) -which is an essential parameter for magnetic refrigeration- using pulsed magnetic fields, are closer to the real process used in applications. The pulse lengths of the non-destructive pulsed-field facilities are in the range 10-100 ms. This agrees well with the targeted operation frequency of the magnetic refrigerators, which is about 10-100 Hz **[6].** Furthermore, the short pulse duration provides nearly adiabatic conditions during the measurement **[7].** A further advantage is that the accessible magnetic field range can easily be extended to beyond 70 T, thus allowing for a thorough characterization of the magnetic properties of a compound also at high fields. The magnetocaloric properties of only a limited number of various types of solids were investigated using this method so far. These include Gadolinium **[8],** Heusler alloys **[9, 10, 11]** and $La(Fe,Si,Co)_{13}$ compounds **[7].** In this work, we study the MCE in a $MnFe_4Si_3$ single crystal by direct magnetocaloric measurements in pulsed magnetic fields and compare the results to the ones obtained by magnetization and specific heat measurements in static magnetic fields.

All compounds of the series $Mn_{5-x}Fe_xSi_3$ possess a hexagonal symmetry at 293 K. According to **[12]** they crystallize in space group *P6₃/mcm* (Figure1 **[13]**). However, a recent structure refinement using x-ray and neutron single crystal diffraction data, led to a new structural model in space group $P\bar{6}$ for the compound $MnFe_4Si_3$, in which Mn and Fe atoms occupy two of the transition metal sites (M1a, M1b) in a partially ordered manner, while the other two sites (M2a, M2b) are completely filled by Fe atoms **[13].**

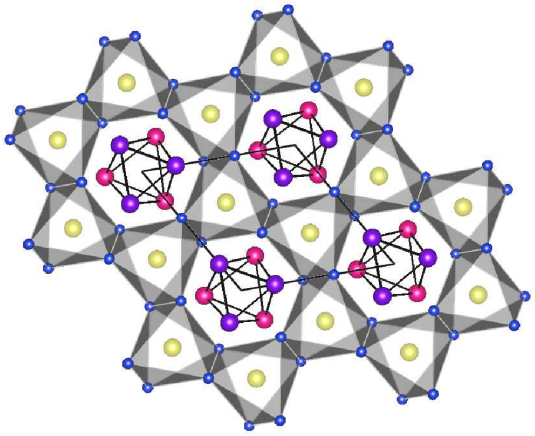

Figure 1. Projection of the structure of $MnFe_4Si_3$ in space group $P\bar{6}$ at 380 K along the [001]-direction [13]. Sites occupied by Mn and Fe are shown in pink (M1a) and magenta (M1b); sites exclusively occupied by Fe are shown in yellow, Si atoms are shown in blue. Pink and magenta sites are in different layers along the [001]-direction. Shortest distances between M1a and M1b sites are indicated in black, and [$FeSi_6$]-octahedra are indicated in grey.

Depending on the stoichiometry, the compounds in the system $Mn_{5-x}Fe_xSi_3$ (x=0-5) undergo various magnetic phase transitions at different temperatures. The magnetic transitions have

been investigated by macroscopic magnetization measurements as a function of temperature on polycrystalline samples **[14, 12].**

Within the system, the compound $MnFe_4Si_3$ is of particular interest as it has a phase transition to a ferromagnetically ordered phase at approximately 300 K **[13, 15].** Macroscopic magnetization measurements showed that this compound has a strong anisotropy of the magnetization (and consequently of the magnetocaloric effect) with the easy axis of magnetization in the *a,b*-plane **[13].** The magnetic entropy change deduced from the hysteresis loops measured on polycrystalline samples using the Maxwell relation has a maximum of −2 J/kgK for a field change of 2 T **[16]** and for single crystal samples a maximum of −2.90 J/kgK for the same field change with the field applied along the *a*-axis, and a smaller value of approx. −1.3 J/kgK with the field applied along the *c*-axis **[13].**

A refinement of the magnetic structure of $MnFe_4Si_3$ in the magnetic space group *Pm'* was carried out based on neutron single crystal data **[13].** It was shown, that the spins on the sites with mixed occupancy of Mn and Fe (M1a/M1b) are aligned in the *a,b*-plane, but it was not possible to refine a significant magnetic moment for the sites exclusively occupied by iron **[9].** As such the compound might be considered as a representative of an MCE material featuring two distinct magnetic sites with different ordering characteristics **[17].**

Even though the MCE in these materials is moderate, the materials could potentially perform well after some optimization through doping. In addition, they are made up of low-cost, abundant and non-toxic elements and they are less brittle compared to competing materials **[18]**. Moreover, it is possible to synthesize these materials as large single crystal, which enables the investigation of the anisotropic magnetic response and magnetic and lattice excitations throughout the Brillouin zone **[19]** to achieve a better understanding of the fundamental mechanism of the MCE.

The aim of this study is to measure and compare the change in isothermal entropy and adiabatic temperature of single crystals of $MnFe_4Si_3$ using static and pulsed magnetic fields in combination with specific heat measurements, and in this way obtaining a detailed picture of the MCE in the material. In addition, the application of pulsed magnetic field provides conditions close to the ones present in real applications and allows obtaining information on the ability of cycling and response time of the studied material.

2. Experimental procedure

Polycrystalline ingots of $MnFe_4Si_3$ were prepared using stoichiometric amounts of the constituent elements (Mn, Fe, and Si). All raw materials were heated under vacuum conditions to remove the impurities and then melted by using cold crucible induction melting under argon atmosphere **[20]**. The resulting product was cooled and the procedure was repeated two times to ensure a high homogeneity of the melt. The obtained polycrystalline sample was cleaned mechanically at the surface to remove any contamination. This polycrystalline material was then used as starting materials for the growth of a large single crystal by the Czochralski method **[21]** in an aluminium oxide crucible using tungsten as seed crystal. Part of the sample was ground in order to confirm the phase purity by X-ray powder

diffractometer. Specimen of different shape and orientation were prepared using a Laue (back-scattering) camera and a spark erosion set-up to match the requirements of the respective investigation method.

The typical size of the crystals used for the magnetization measurements was of several cubic millimetres. For the direct measurements of the magnetocaloric effect plate-like samples were cut with the size 5x5x1 mm, with the plane cut normal the [100] and [001] crystallographic directions.

The samples have been characterized in-house performing magnetization measurements and heat capacity measurements in static fields using the vibrating sample magnetometer (VSM) and the thermal relaxation calorimeter of Quantum Design PPMS and PPMS Dynacool, respectively.

We have performed isothermal magnetization measurements always starting the measurement at maximum field. Temperature dependences shown here are derived from the isotherms filtering the data for the same applied field and the same field history. In the heat capacity measurements, the sample was fixed to the platform (with the a-axis aligned parallel to the magnetic field) using silver paint to assure a good thermal contact between the puck platform and the sample (Figure2 (right)).

Pulsed-field magnetization measurements were performed at Dresden High Magnetic Field Laboratory (HLD-EMFL) using the induction magnetometer with a pulse length of 50 ms and up to 35 T for the hard direction and up to 8.5 T for the easy direction **[22].** Both measurements were done at a temperature of 4.2 K.

The direct measurements of the MCE were also performed at HLD. The temperature change of the sample was monitored by a Copper-Constantan thermocouple sandwiched between two sample plates to optimize the thermal contact and reduce the heat losses. A resistive Cernox thermometer was utilized to determine the reference temperature (Figure2 (left, middle)).

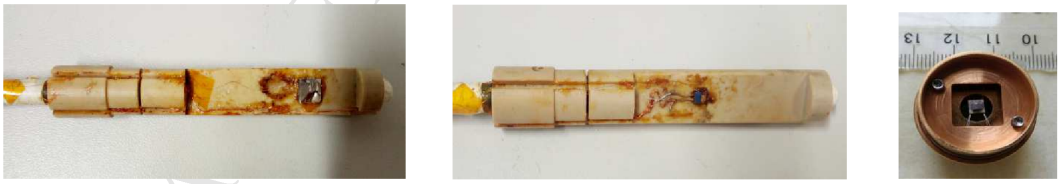

Figure 2: The holder for the direct measurements of the MCE with the samples mounted on it (left), the back side of the holder with the reference junction installed (middle) and the holder for the heat capacity measurements with the sample on it (right)

3. Results and discussion

The phase purity of the ground single crystal was confirmed by x-ray powder diffraction (Fig.S1). A LeBail refinement **[23]** performed with the program Jana 2006 **[24]** yielded

lattice parameters a = 6.802(1) Å and c = 4.7293(7) Å in good agreement with the literature values (a = 6.8057(2) Å and c = 4.72965(16) Å **[13]**).

3.1 Magnetization measurements in static and pulsed fields

Figure 3 shows the magnetization of $MnFe_4Si_3$ as a function of the applied magnetic field M(H) parallel to the crystallographic a-axis (top left) and parallel to the crystallographic c-axis (top right). A clear anisotropy of the magnetic response can be seen.

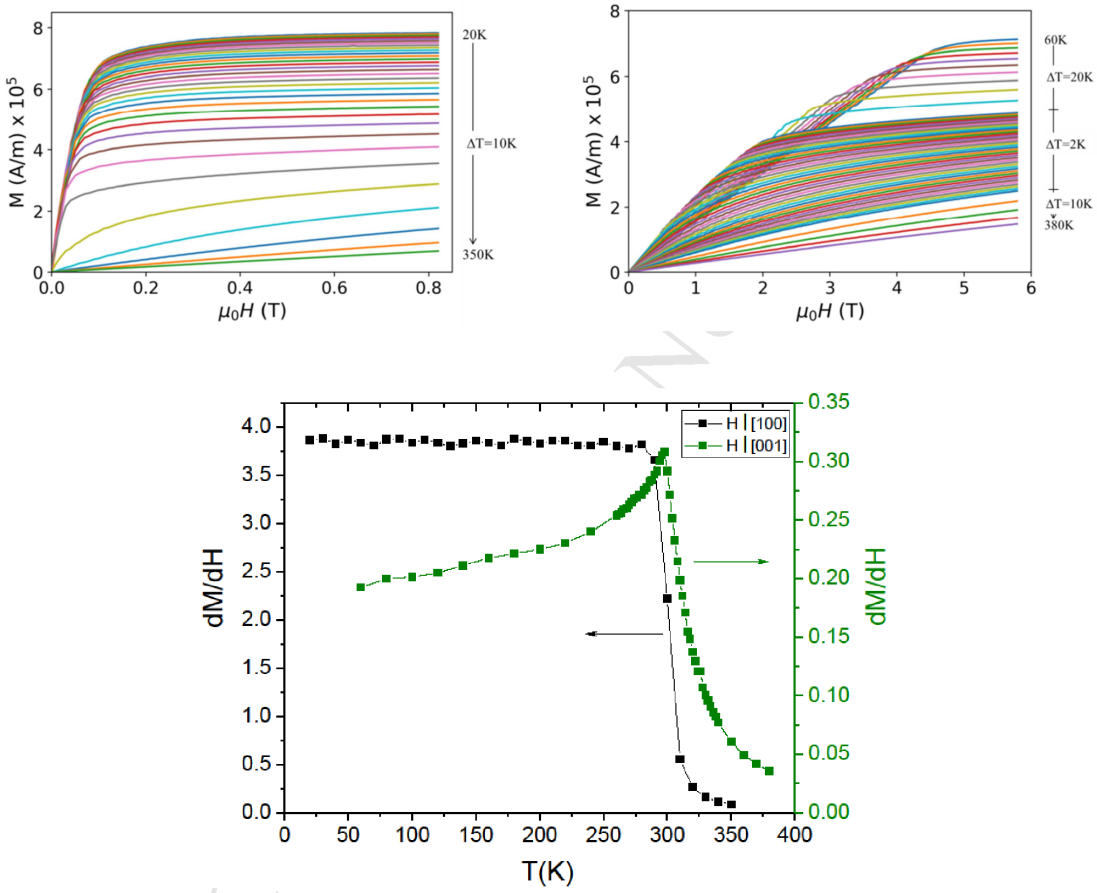

Figure 3. Magnetization curves of $MnFe_4Si_3$ for the magnetic field applied parallel to [100] (top left) and to [001] (top right) at different initial temperatures. dM/dH in the region around zero field, H ∥ [100] and H ∥ [001] (bottom). Statistical error bars are typically smaller than the symbols size.

To take the demagnetization into account we used the demagnetization factor for rectangular prisms tabulated in **[25]**. It should be noted that the specimen for the easy axis measurements has an irregular shape, hence introducing a small systematic error.

After the correction one can still observe linear field dependence at small fields (albeit less steep with the field in [001] than with the field along [100]) in the ordered phase, followed by a saturation region. Each curve was fitted with a linear function in the respective regions. On

the basis of these data, dM/dH in the region around zero field was calculated (figure 3, bottom).

For the data with H ‖ [100], the slope is constant at low temperatures within the magnetically ordered state. For temperatures below 300 K, the magnetization is saturated already for μ_0H=0.4 T. At 20 K the saturation moment reaches 117.35(1) Am^2/Kg at a field of 0.4 T. For higher fields, there is a small linear increase. Upon increasing the temperature, the sharp transition is gradually broadened and the value of saturation magnetization decreases. Close to the transition temperature, the slope at small fields changes drastically and the saturation is not reached at 1 T (top right). At 330 K and above, the magnetic moment increases linearly with the field in the measured range and the sample shows a paramagnetic behaviour. Comparing with the results from **[13]**, in general a good agreement can be seen with only slightly smaller values of the maximum magnetization and the field of saturation in the results presented here.

For the data with H ‖ [001] the magnetic response is different to the case with H ‖ [100]. The field dependence of magnetization increases slower and reaches smaller maxima compared to the measurement with H ‖ [100]: the magnetization reaches about 109.87(3) Am^2/Kg at a field of 5 T at 60 K. All these observations clearly confirm that for $MnFe_4Si_3$, the easy axis of magnetization is in the *a,b*-plane and the *c*-direction is the hard axis of magnetization. At higher fields, there is a small linear increase and up to 6 T there is no clear saturation. This agrees with earlier results **[13]**, where no saturation was reached in a field up to 4 T. Above 300 K, the magnetization dependence the magnetic response within the probed field range becomes more and more linear.

dM/dH exhibits distinct features for the different field directions. For the [100] direction it increases until the temperature approaches the transition temperature after that it remains nearly constant. Along the hard direction, dM/dH features a sharp maximum at the transition temperature. The presence of the maximum results also in a sign change of the magnetic entropy change as discussed below.

For the calculation of the MCE from the magnetization curves, we determine dM/dT by extraction of respective M(T,H) from the respective isotherms (Fig.S2). Figure 4 displays the isothermal entropy change ΔS_M calculated via the Maxwell relation:

$$\Delta S_M(T,\Delta H) = \int_{H1}^{H2} \left(\frac{\partial M(T,H)}{\partial T}\right) dH \quad \text{.....(2)}$$

The magnetocaloric effect has a maximum value at approximately 300 K and from the curves it is obvious that it shows a significant anisotropy. With an applied field along the *a*-axis, the magnetic entropy change has a maximum of about 1.3 J/kgK for a field change of 1 T, compared to a magnetic entropy change of about 3.5 J/kgK for a field change of 6 T with the field along the *c*-axis. The entropy change for the field applied ‖ [100] is consistent with the earlier results from single crystal **[13]** and powder measurements **[16].** The entropy change for small field changes of 1T applied along the hard direction reveals a more complex behaviour (the orange curve in figure 4). Here, one observes an inverse MCE around 280 K

where ΔS_{mag} is positive. With further temperature increase the sign changes. And the inverse MCE is suppressed for larger field changes and increases stronger than linear with field. These observations demonstrate that the MCE in this compound is clearly dominated by the magnetic moments aligned in the *a*,*b*-plane.

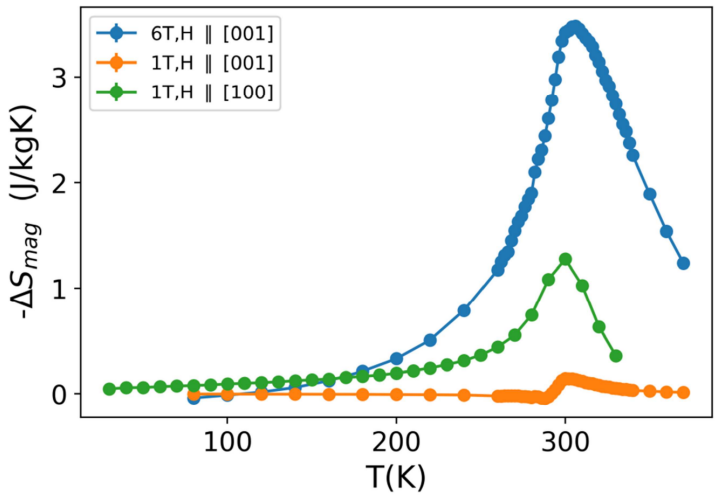

Figure 4. MCE of $MnFe_4Si_3$ calculated from magnetization data at a field of 1 T for H‖ [100] (green curve) and at a field of 1 and 6 T for H‖ [001] (orange and blue curves respectively).

Figure 5 shows the field dependent magnetization M(H) obtained from the pulsed magnetic field experiment together with isothermal magnetization data measured in a field up to 8 T in the [100] direction and up to 35 T in the [001] direction at 5 K. The pulsed field magnetization measurement data was normalized to the DC field data at 8 T in the first direction and to the data at 8.5 T in the other direction.

It can be seen that there is a good match between the curves. Magnetization curve along the hard [001] direction reaches saturation at about 5.5 Tesla. No further evolution of magnetization was discovered up to the highest fields.

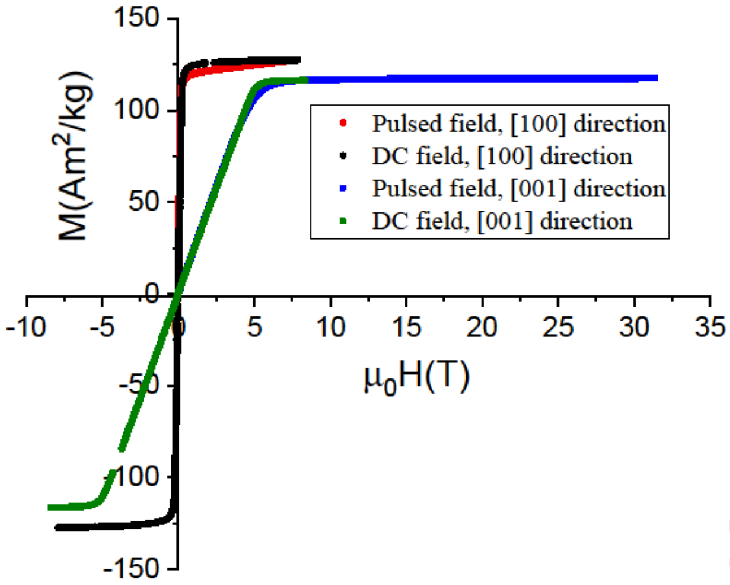

Figure 5. M(H) curves in pulsed magnetic field and DC field at 5 K in [100] direction and [001] direction.

3.2 Direct measurements of ΔT_{ad} in pulsed magnetic fields

Figure 6 shows the field dependence of the adiabatic temperature change for a field change of 2 T (top) and 20 T (bottom) applied along [100] direction at 310 K. From the figures it is clear that the magnetization and demagnetization curves nearly coincide, (the short pulse time is not detrimental for the response time of the thermocouple) which underscores the ability of cycling of these measurements (adiabatic condition). For the other temperatures, the curves are looking the same (Fig.S3).

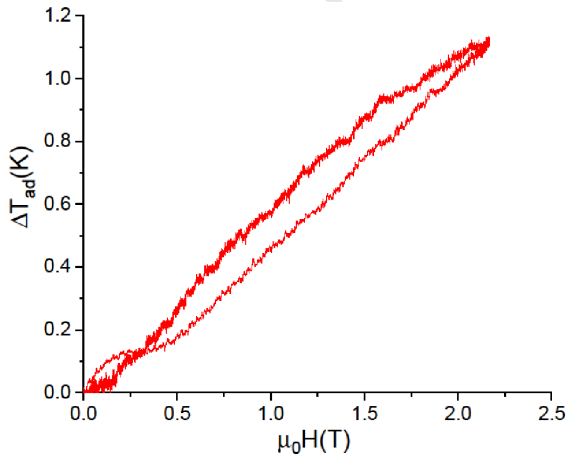

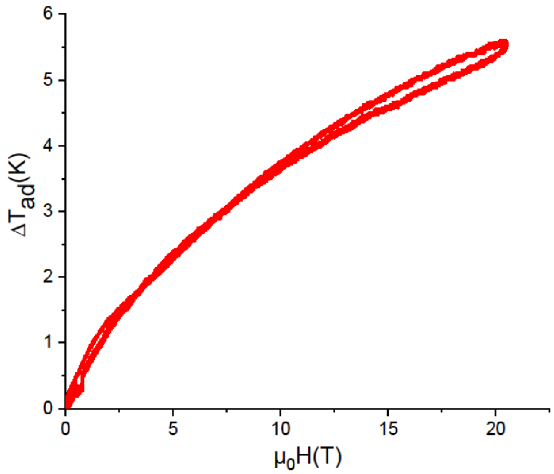

Figure 6. Field dependence of ΔT_{ad} for a pulsed field change of 2 T (top) and 20 T (bottom) applied along [100] direction at 310 K. The readout from the temperature sensor was averaged over 15 points and shifted to start from the origin.

Figure 7 shows the adiabatic temperature change for the easy direction of a $MnFe_4Si_3$ single crystal sample as obtained from the direct measurements in pulsed magnetic field up to 2 T (black symbols) and 20 T (blue symbols). It is obvious that ΔT_{ad} increases with increasing the applied magnetic field. A maximum ΔT_{ad} occurs at T_C (300 K) for a field change of 2 T. With increasing the magnetic field up to 20 T, the observed peak broadens and shifts towards higher temperatures, as the transition into the paramagnetic state broadens upon the application of the magnetic field. As the magnetic field stabilizes the ferromagnetic order, a higher thermal energy is needed to bring the system into a higher entropy state and hence the maximum adiabatic temperature change happens at higher temperature. This broad maximum is also reported in **[26]** for the $La(Fe,Si)_{13}$ system and for the $La(Fe,Si,Co)_{13}$ system **[7].**

The maximum values of ΔT_{ad} are 1.38 and 5.66 K for field changes of 2 T and 20 T, respectively. Thus, the adiabatic temperature change increases only by a factor of 4 although the field is increased by a factor 10. Similarly, ΔT_{ad} for a pulsed field up to 50 T at 320 K gave an increase of ΔT_{ad} up to a value of 9.45 K.

By using the relation (1), the change in the adiabatic temperature was calculated for different initial temperatures from the magnetization and heat capacity measurement for a field change of 2 T (see the curve in Fig.S4 for ΔS values and the black curve in figure 9 for C(p,H) values). A comparison with the values from the direct measurements in pulsed fields of 2 T (red and black curves in figure 7) shows good agreement. From the indirect measurements we got a maximum of 1.21 K at 305 K and a field change of 2 T compared to a maximum value of 1.38 K from the direct measurements at 300 K and a field change of 2 T. The slight deviation of the maximum temperature and value can be explained by the coarse temperature steps of the isothermal measurements, which systematically affects the numerical approximation to eq. (2).

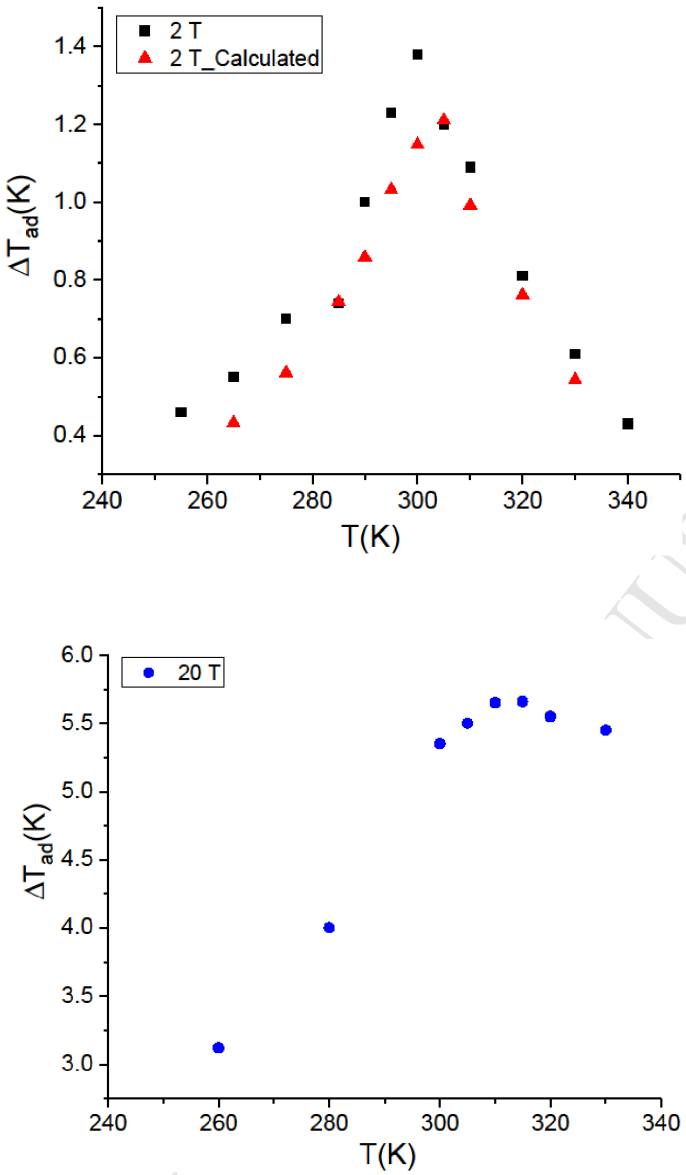

Figure 7. Comparison of ΔT_{ad} for the easy direction measured in pulsed magnetic fields of 2 T (black symbols) and calculated from the magnetization and heat capacity measurements in static magnetic fields of 2 T (red symbols, top). ΔT_{ad} measured in pulsed magnetic fields of 20 T (blue symbols, bottom).

Figure 8 shows a comparison between the time dependences of the adiabatic temperature change in pulsed magnetic field of 20 T applied in [100] direction at 330 K (left) and the time dependences of trial measurement of ΔT_{ad} in a field of 10 T applied in the [001] direction at 340 K (right). For the easy direction [100], the pulsed field profile and the measured temperature change nearly coincide. On the other hand, for the measurements with the field applied in [001] direction, the temperature signal of the thermocouple lags the field pulse significantly, see right panel in Fig. 8. This and the finite signal of the thermocouple before

the pulse can be attributed to a small open loop of the thermocouple wires, despite a careful twisting of the wires during the sample preparation. In addition, an artificial sharp maximum (Fig.S5, +10 T and -10 T curves) appears at the beginning of the $\Delta T_{ad}(t)$ curve. To cancel this contribution, two measurements taken at positive and negative field have been averaged. The measured data indicate that the temperature change with the field applied in the [001]-direction is considerably lower than the one with the field applied in the easy direction.

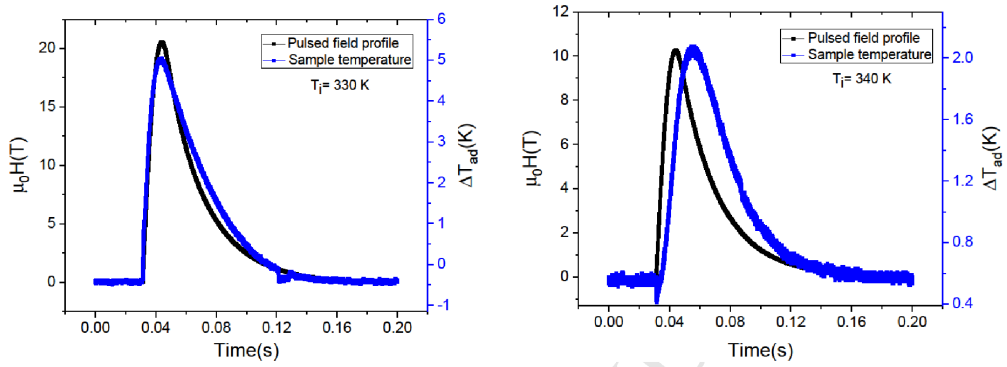

Figure 8. Time dependences of the adiabatic temperature change in pulsed magnetic field of 20 T in [100] direction at 330 K (left) and time dependences of ΔT_{ad} in pulsed magnetic field of 10 T in [001] direction at 340 K (right). For the data with the magnetic field in [001], two measurements with positive and negative field were averaged.

3.3 Heat capacity measurements

The temperature-dependent heat capacity data of $MnFe_4Si_3$ measured at a magnetic field of 0, 1 and 2 T (Figure 9), show only small differences in the temperature region between 2-280 K. In zero fields we can then clearly identify a lambda anomaly related to the magnetic phase transition. It can be noted, that the peak of the lambda anomaly rather coincides in temperature with the peak in the magnetic susceptibility for the field ǁ [001].

Upon application of a magnetic field, the anomaly broadens and shifts towards higher temperature as expected. We observe, however, further features at elevated temperatures above the phase transition at ~320 K and 350 K. These are pronounced in the 0 T and 1 T data, but smeared out in the 2 T data. Only at 380 K – 400 K the three curves merge again, nearly 100 K above the magnetic phase transition. It is noteworthy that in earlier investigation by resonant ultrasound spectroscopy **[16]** it was also observed that the effects of the magnetic field extended well above the transition temperature, a fact that was ascribed to the strong response of the lattice to a magnetic field.

Clearly the field dependent lattice dynamics needs to be addressed for a better understanding of the MCE in $MnFe_4Si_3$, yet this exceeds the scope of this paper.

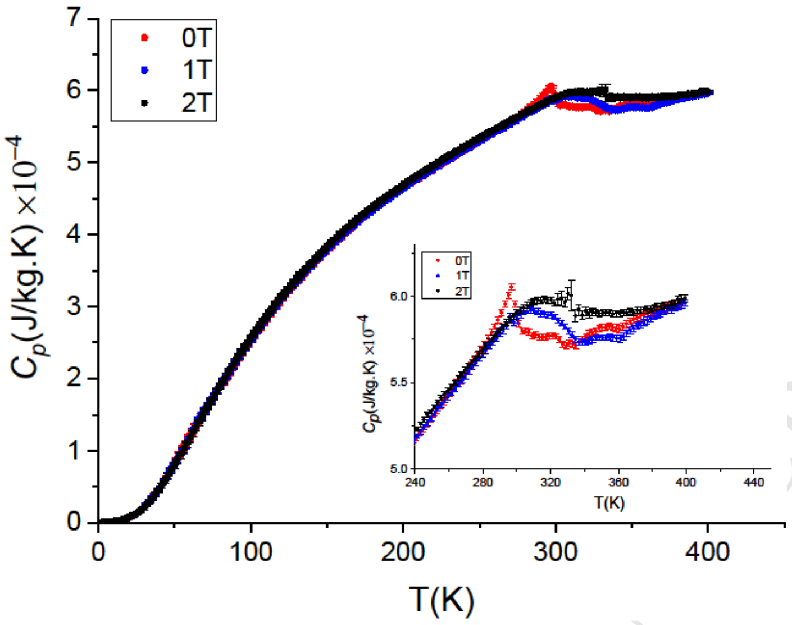

Figure9. Temperature-dependent heat capacity data of $MnFe_4Si_3$ measured at 0, 1 and 2 T. The broad maximum around room temperature corresponds to the magnetocaloric effect.

4. Conclusions

The magnetic and magnetocaloric properties of single crystalline $MnFe_4Si_3$ were studied. The magnetization and MCE were measured in both constant and pulsed fields. As a strong magnetic anisotropy was observed, the measurements were done with an applied field along [100] direction and along [001] direction.

Magnetization measurements in DC fields confirm that the easy axis of magnetization lies in the *a*,*b*-plane. The field dependence of the magnetic moments shows that the compound undergoes a first-order phase transition to a ferromagnetic ordered phase at approximately 300 K. Due to the good agreement of the shape of the magnetization curves in static and pulsed field we could use the static measurements to calibrate the pulsed field data. These in turn provided the information that no further transition appears up to very large fields.

Direct and indirect measurements of MCE are in a really good agreement, so direct measurements could be used to address the anisotropy of MCE as well. In particular $MnFe_4Si_3$ runs very cyclable through the pulsed cycles, which might be an important property in terms of potential applications. The good stability and the ability of cycling might be related to the fact that the lattice reacts dynamically to the magnetic ordering and not by discontinuous structural changes **[13]**. However, here we can only speculate about the relation between lattice dynamics and magnetic structure and a thorough investigation of the phonon spectrum as a function of the magnetic field is needed to gain further insight.

Acknowledgements

This work is part of a collaborative agreement between the Forschungszentrum Jülich and Al-Quds University and was supported by the BMBF under the programme *Zusammenarbeit mit Entwicklungs- und Schwellenländern im Nahen Osten, Nordafrika, Türkei* (Project MagCal, 01DH17013) and under the Joint Research and Education Programme *Palestinian German Science Bridge PGSB*. The work is based upon experiments performed at HLD at HZDR, member of the European Magnetic Field Laboratory (EMFL). Two of the authors (KF and MGH) acknowledge financial support by the German Science Foundation (SFB917 Nanoswitches).

References

[1] C.B. Zimm, A. Jastrab, A. Sternberg, V. Pecharsky, K.A. Geschneidner Jr., M. Osborne and I. Anderson, *Description and Performance of a Near-Room Temperature Magnetic Refrigerator,* Adv. Cryogenic Engineering, 43, (1998).

[2] K.A. Gschneidner Jr. and V.K. Pecharsky, *Thirty years of near room temperature magnetic cooling: Where we are today and future prospects*, Int. J. Refrig., 31, 945 – 961 (2008).

[3] B.F. Yu, Q. Gao, B. Zhang, X.Z. Meng and Z. Chen, *Review on research of room temperature magnetic refrigeration,* Intl. J. Refrig., 26, 622 – 636 (2003).

[4] V.K. Pecharsky and K.A. Gschneidner Jr., *Magnetic refrigeration material*, J. Appl. Phys.,85, 5365 (1999).

[5] M. Foldeaki, R. Chahine, and T.K. Bose,*Magnetic measurements: A powerful tool in magnetic refrigerator design,* J. Appl. Phys., 77, 3528 (1995).

[6] M.D. Kuz'min, *Factors limiting the operation frequency of magnetic refrigerators,* Appl. Phys. Lett., 90, 251916 (2007).

[7] M. Ghorbani Zavareh, Y. Skourski, K. P. Skokov, D. Yu. Karpenkov, L. Zvyagina, A. Waske, D. Haskel, M. Zhernenkov, J. Wosnitza, and O. Gutfleisch, *Direct Measurement of the Magnetocaloric Effect in La(Fe,Si,Co)$_{13}$ Compounds in Pulsed Magnetic Fields,* Phys. Rev. Applied 8, 014037 (2017).

[8] T. Gottschall, M. D. Kuz'min, K. P. Skokov, Y. Skourski, M. Fries, O. Gutfleisch, M. Ghorbani Zavareh, D. L. Schlagel, Y. Mudryk, V. Pecharsky and J. Wosnitza, *Magnetocaloric effect of gadolinium in high magnetic fields*, Phys. Rev. 99, 134429 (2019).

[9] M. Ghorbani Zavareh, C. Salazar Mejía, A. K. Nayak, Y. Skourski, J. Wosnitza, C. Felser and M. Nicklas, *Direct measurements of the magnetocaloric effect in pulsed magnetic fields: The example of the Heusler alloy $Ni_{50}Mn_{35}In_{15}$*, Appl. Phys. Lett. 106, 071904 (2015).

[10] C. Salazar-Mejía, V. Kumar, C. Felser, Y. Skourski, J. Wosnitza and A.K. Nayak, *Measurement-Protocol Dependence of the Magnetocaloric Effect in Ni-Co-Mn-Sb Heusler Alloys,* Phys. Rev. Applied11, 054006 (2019).

[11] P. Devi, M. Ghorbani Zavareh, C. Salazar Mejía, K. Hofmann, B. Albert, C. Felser, M. Nicklas and Sanjay Singh, *Reversible adiabatic temperature change in the shape memory Heusler alloy $Ni_{2.2}Mn_{0.8}Ga$:An effect of structural compatibility,* Phys. Rev. Materials 2, 122401(2018).

[12] H. Binczycka, Z. Dimitrijevic, B. Gajid and A. Szytuu, *Atomic and Magnetic Structure of $Mn_{5-x}Fe_xSi_3$*, phys. Stat. sol.,19, K13 (1973).

[13] P. Hering, K. Friese, J. Voigt, J. Persson, N. Aliouane, A. Grzechnik, A. Senyshyn and T. Brückel, *Structure, Magnetism, and the Magnetocaloric Effect of $MnFe_4Si_3$ Single Crystals and Powder Samples*, Chem. Materials, 27, 7128-7136 (2015).

[14] Songlin, Dagula, O. Tegus, E. Bruck, J.C.P. Klaasse, F.R. de Br, and K.H. J. Buschow, *Magnetic phase transition and magnetocaloric effect in $Mn_{5-x}Fe_xSi_3$*, J. Alloys Compounds, 334, 249–252 (2002).

[15] O. Gourdon, M. Gottschlich, J. Persson, C. de la Cruz, V. Petricek, M. A. McGuire and T. Bruckel, *Toward a better understanding of the magnetocaloric effect: An experimental and theoretical study of $MnFe_4Si_3$*, J. Solid State Chem., 216, 56−64 (2014).

[16] M. Herlitschke, B. Klobes, I. Sergueev, P. Hering, J. Perßon, and R. P. Hermann, *Elasticity and magnetocaloric effect in $MnFe_4Si_3$*, Phys. Rev., B93, 094304 (2016).

[17] L. Caron, N. Ba Doan and L. Ranno, *On entropy change measurements around first order phase transitions in caloric materials,* J. Phys.: Condens. Matter 29, 075401 (2017).

[18] K. A. Gschneidner Jr, V. K. Pecharsky and A. O. Tsokol, Recent developments in magnetocaloric materials, Rep. Prog. Phys 68, 1479–1539 (2005).

[19] N. Biniskos, S. Raymond, K. Schmalzl, A. Schneidewind, J. Voigt, R. Georgii, P. Hering, J. Persson, K. Friese, and T. Brückel, *Spin dynamics of the magnetocaloric compound $MnFe_4Si_3$*, Phys. Rev., B 96, 104407 (2017)

[20] S.V. Stefanovsky, S.V. Yudintsev, S.E. Vinokurov and, B.F. Myasoedov, *Chemical-Technological and Mineralogical-Geochemical Aspects of the Radioactive Waste Management,* Geochemistry International (2016).

[21] J. Czochralski, *A new method for the measurement of the crystallization rate of metals*, Z. Phys. Chem., 92, 219–221 (1918).

[22] Y. Skourski, M.D. Kuz'min, K.P. Skokov, A.V. Andreev and J.Wosnitza, *High-fieldmagnetization of Ho_2Fe_{17}*, Phys. Rev., B 83, 214420 (2011).

[23] D.H. Le Bail, A. and J. L. Fourquet, *Ab-initio structure determination of $LiSbWO_6$ by X-Ray powder diffraction,* Mat. Res. Bull., 23, 447-452 (1988).

[24] V. Petricek, M. Dusek and L. Palatinus, *Jana2006 Crystallographic computing system for standard and modulated structures,* Version 30/11/2014 (2006).

[25] D.-X. Chen, E. Pardo and A. Sanchez, *Demagnetizing Factors of Rectangular Prisms and Ellipsoids*, IEEE Trans. Magn., vol. 38, 4(2002).

[26] S. Fujieda, A. Fujita and K. Fukamichi, *Large magnetocaloric effect in $La(Fe_xSi_{1-x})_{13}$ itinerant-electron metamagnetic compounds*, Appl. Phys. Lett., 81, 1276 (2002).

Supplementary Materials

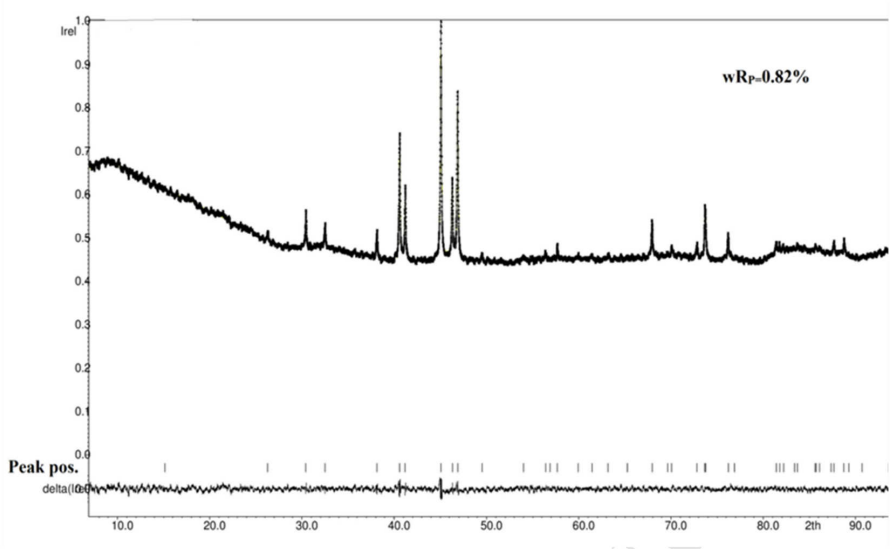

Fig.S1: Observed intensities and the difference profile of $MnFe_4Si_3$ measured at room temperature from the LeBail refinement.

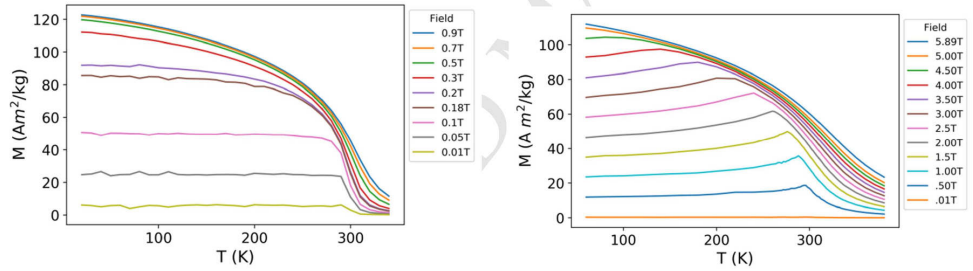

Fig.S2. Temperature-dependent magnetization of $MnFe_4Si_3$ from hysteresis measurements, for H ‖ [100] (left) and H ‖ [001] (right).

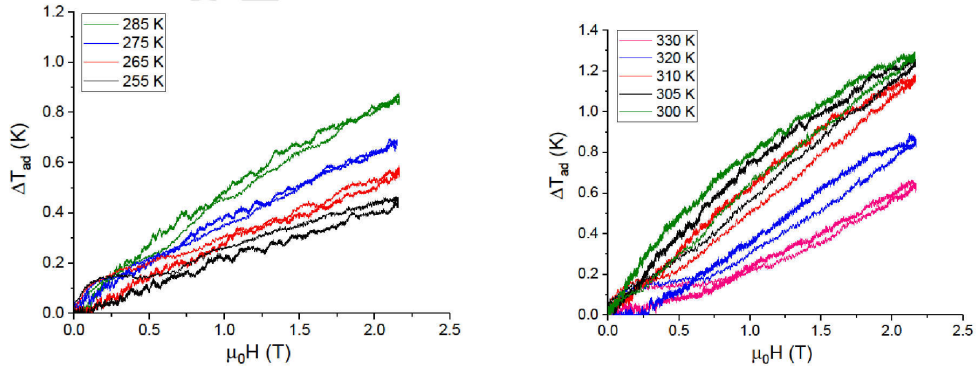

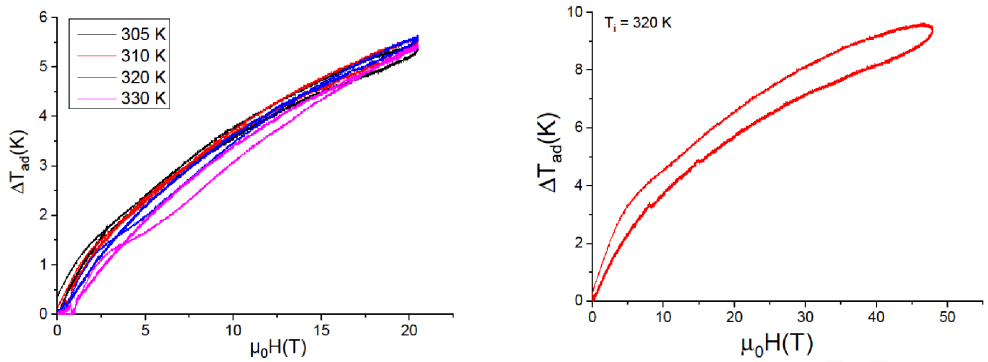

Fig.S3: field dependence of ΔT_{ad} for different initial temperatures and a pulsed field change of 2 T, 20 T and 50 T.

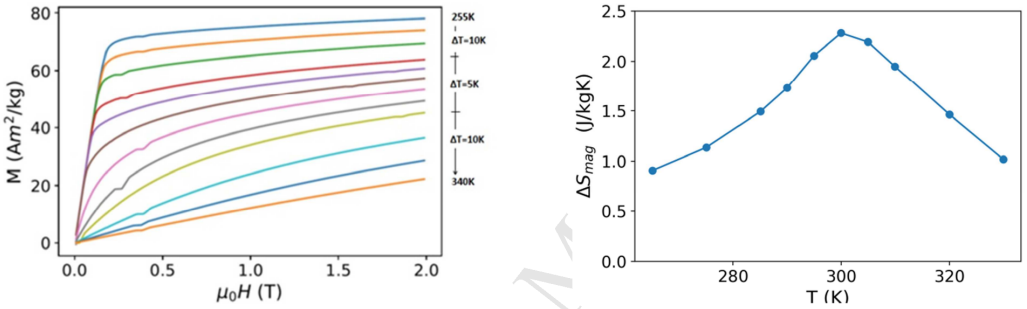

Fig.S4. Magnetization curves of $MnFe_4Si_3$ showing the magnetization as a function of the applied magnetic field parallel to [100] (left), MCE of $MnFe_4Si_3$ calculated from the magnetization data at a field of 2 T, H ‖ [100].

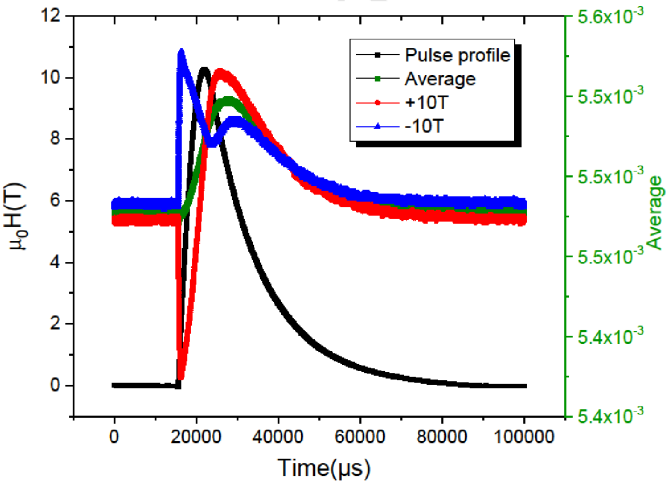

Fig.S5: Time dependence of the raw signal with pulsed fields of +10 T and -10 T at 340 K and the average of them two.

Highlights:

- Direct measurement of the adiabatic temperature change using pulsed magnetic fields is an excellent technique for the evaluation of the magnetocaloric effect, as it provides nearly adiabatic conditions and an experimental situation that is close to the one present in real applications.

- The compound $MnFe_4Si_3$ shows high cyclability even in very high fields which confirms its high structural stability against field changes, an important property for applications."